Asynchronous measurments and control : a case study on motor synchronisation

Eindhoven University of Technology
Department of Electrical Engineering

Asynchronous measurements and control: a case study on motor synchronisation

W.P.M.H. Heemels, R.J.A. Gorter,
A. van Zijl, P.P.J. van den Bosch,
S. Weiland and M.R. Vonder

June 1998

Measurement and Control Systems
Internal Report, 98 I/03

Paper submitted for publication elsewhere

Eindhoven, June 1998

Asynchronous measurement and control: a case study on motor synchronisation

Running title: Asynchronous measurement and control

W.P.M.H. Heemels[†], **R.J.A. Gorter**[‡], **A. van Zijl**,
P.P.J. van den Bosch, **S. Weiland**
Eindhoven University of Technology, Dept. of Electrical Engineering
P.O. Box 513, 5600 MB Eindhoven, The Netherlands

[†] corresponding author, email: w.p.m.h.heemels@ele.tue.nl, fax: +31 40 2434582

[‡] Currently at TNO-Industry, Dept. of Product Development
P.O. Box 5073, 2600 GB Delft, The Netherlands

M.R. Vonder
Buhrs-Zaandam B.V.
P.O. Box 92, 1500 EB Zaandam, The Netherlands

June 19, 1998

Abstract

In this paper the synchronisation between two or more electrical motors (a master and one or more slaves) is studied. To reduce the costs of the master-slaves combination, the slave motors are mounted with a very low resolution encoder (one or several pulses per revolution). The low resolution of the slave encoders has severe consequences on the control algorithm. Two methods are proposed to deal with the low resolution encoders: the hybrid and the asynchronous control scheme. In the hybrid scheme the measurement is updated at the time that slave position information is available, the control is updated at a fixed time rate. In the asynchronous scheme, both the measurement and the control value are updated only at the time the slave position becomes available. Since the sample times are now determined by state-events (a system variable crossing certain values), standard control and analysis techniques are not applicable. For the asynchronous controller a new design technique is proposed. The presented controllers are tested successfully on a real industrial master-multi-slave system as is used in mailing machines.

Keywords: master-slave system, synchronization, encoders, motor control, industrial production systems, discrete event dynamic systems.

1 Introduction

Machines often contain several electrical motors whose motions have to be coordinated. A situation that one frequently encounters is that the position of several motors (the slaves) should follow the position of a master motor. Examples of such applications are product handling machines and multi-conveyor-belt-systems. Traditionally, this kind of synchronization is achieved with one mechanical axis that drives all the tools. Nowadays, these mechanical axes are replaced by one or more 'electrical axes' to obtain more flexibility in the sense that tools can easily be added or removed (plug and play concept). With an electrical axis, a small motor is connected to each tool separately and electronic control is used to synchronise the tools (slaves) with respect to a master. The motors of these machines often drive different loads which makes synchronisation difficult.

The position of the electrical motor is measured by an encoder, which gives pulses only at fixed positions of the motor axis. Hence, the times at which information about the motor axis position becomes available are not equally spaced in time and are, in fact, triggered by state-events (a systems variable crossing a certain threshold, cf. Figure 2 below). These encoders usually have a high resolution, typically 1000 to 5000 individual measured positions (pulses) per revolution of the motor axis. In practice, these high resolution encoders are read out after fixed time intervals and the state-event character of the encoder is neglected.

The company Buhrs-Zaandam B.V. also uses these high resolution encoders. This company builds mailing systems which automatically compose a mailing consisting of several brochures. A mailing system is depicted in Figure 1. The main component of the mailing (e.g. book or magazine) enters the conveyor belt (lug chain) at the loadermodule (1 in Figure 1). Several supplements are added to the main product by a feedermodule consisting (in this particular case) of three sheet-feeders (2). Sheet-feeders basically grip a brochure from a stack and throw this on a conveyor belt (the master in this case). The main product together with the supplements form a package that is wrapped in plastic foil by a packaging module (3). The foil is being supplied by a reel stand (4). Incorrect packages are removed at the rejectionmodule (5). Finally, the product is released after which an address is printed on it, using a label or directly, via an inkjet printer (6). After this the product is put on a stack (7). In such a mailing system many slave motors are present and only one master. It is obvious that synchronisation is required.

To reduce the total costs of a mailing system Buhrs-Zaandam raised the question whether it is possible to replace the expensive high resolution encoders of the slaves by cheap low resolution encoders (with 1 to 8 measurements per revolution of the motor axis) without loosing tight synchronisation between the conveyor belt and the sheet-feeders. With these low resolutions it is no longer possible to neglect the state-event character of the sensors. Buhrs-Zaandam provided a test set-up to re-examine and validate control algorithms for the synchronisation of master and slave motors. The test set-up consists of two induction motors in which one of the motors drives a sheet-feeder.

Control based on state-event sensors is essentially different from systems with high resolution sensors or sensors which operate at a fixed sample rate. In the literature, sampled-data systems are conventionally treated by either standard continuous-time or discrete-time methods. In

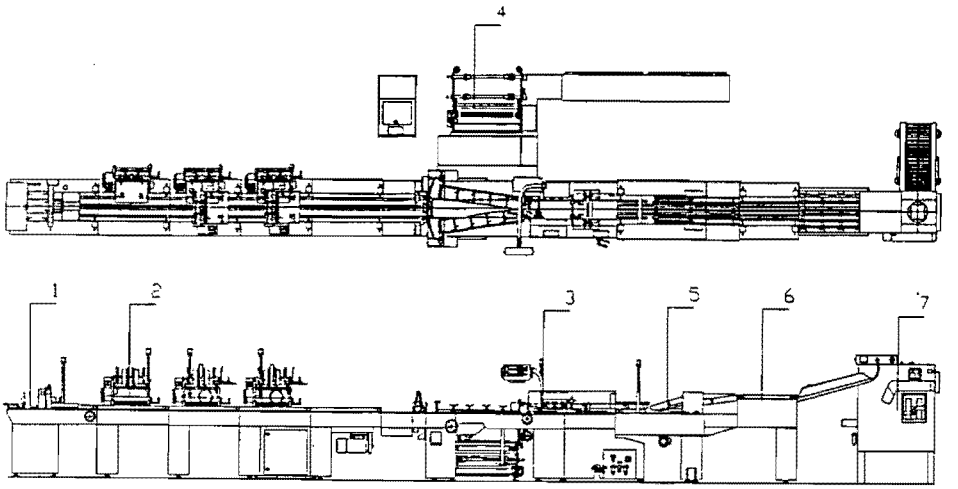

Figure 1: Mailing system.

continuous-time control one assumes that the sampling frequency is high enough compared with the desired bandwidth of the closed-loop system. The designed continuous-time controller is then discretized based on the sampling frequency. In discrete-time control, the system is described by a discrete-time plant and one designs a discrete controller irrespective of the intersample behaviour of the original continuous plant. However, there are also approaches that result in discrete-time controllers that are optimal with continuous-time performance criteria (see e.g. Bamieh and Pearson (1992)). Bamieh and Pearson (1992) deals with single rate control, which means that the sampling frequency is equal to the rate of update of the control signal. The problem of multirate control is studied for instance in Chen and Qiu (1994), Voulgaris (1993) and Sågfors and Toivonen (1997). In the context of motor control with reasonably low resolution encoders, Hori et al. (1991) and Chiang (1990) propose a multirate scheme, where the control rate is high to prevent long deadtime in the control action and the read-out rate of the encoder is constant, but much smaller than the control rate to prevent large quantization errors in the estimation of the speed.

The common feature of these references (and the references therein) is that the times of control update and measurements are known a priori. Stated otherwise, the control and sampling rates are fixed and the sampling times are equally spaced along the time axis. Both updates are based on *time-events*: if a certain time elapses a measurement comes in or/and a control may be updated. In contrast with this, one often encounters sensors that provide new measurement not at fixed time instants, but at fixed "positions." Besides the example of the motor/encoder system, this feature also applies to level sensors for measuring the hight of a fluid in a tank, (magnetic/optic) disk drives with similar measurement devices, transportation systems where the longitudinal position is only known when a marker has passed, etc.

The large literature on sampled-data control hardly addresses sampling based on state-events. The only approach to the problem with state-event sensors known to the authors is described in Philips and Tomizuka (1995). In this paper a discrete-time controller with a fixed control rate is designed based on a state observer with asynchronous updates, i.e. not equally spaced in

time. The state observer is based on a time-varying Luenberger observer and uses the model to estimate the state of the system between two measurements. This calls for fast processors, since on-line calculation of matrix exponentials and time varying Luenberger gains is required at every state-event. Furthermore, Philips and Tomizuka do not consider systems involving (substantial) disturbances. In the presence of disturbance, the approach of estimating the behaviour in between measurements would become unreliable unless information on the disturbances is known and incorporated. This would result in more complex control structures.

In this paper, some alternative approaches will be presented yielding simpler control structures. The general problem on how to control systems with state-event sensors will not be solved here. However, two methods will be proposed which have successfully been implemented for the synchronization of a master motor and a sheet-feeder. The ideas presented here may give a first approach on how to solve the general problem. Although the analysis may seem difficult, the actual implementations are simple and meet the specifications.

The first approach is based on updating the position error estimate between master and slave only at time instants that a new slave position measurement becomes available. In between the measurements the position error estimate is held constant. The control action is still updated at a fixed rate. Due to this mixed character, this control scheme is called 'hybrid.' In the second method, the idea of a constant control rate is abandoned and the control is updated at the time a new position measurement is available. For this 'asynchronous' controller, the standard tools for control design no longer apply as the updates are asynchronous in time. However, this asynchronous control problem for a linear plant is transformed into a synchronous control problem for a nonlinear plant for which a discrete controller can be designed using standard methods.

Both methods (hybrid and asynchronous) have been tested on the experimental set-up and lead to satisfactory performance for a mailing system, when encoder resolutions are used as low as 1 pulse per revolution of the slave motor axis.

The outline of the paper is as follows. After introducing the problem formulation in section 2, the performance is evaluated that can be obtained with a standard discrete-time PID-controller with a fixed sample rate. It is shown that with decreasing encoder resolutions, the controller performance rapidly deteriorates and becomes unacceptable. In section 4 the advantages of using asynchronous measurements is explained. The required new control techniques are treated in sections 5 and 6. In section 7 additional tests like starting up the mailing system are carried out. Finally, in section 8 the conclusions are stated.

2 Problem formulation

In this section, the general problem and the details of the test set-up are introduced.

2.1 Basic problem

Consider a linear time-invariant plant

$$\dot{x}(t) = Ax(t) + Bu(t) + Ed(t) \tag{1}$$

with $x(t)$, $u(t)$ and $d(t)$ the state, control and disturbance, respectively, at time t. A, B, E are constant real matrices of appropriate dimension. The measurements are given by

$$y(t) = Cx(t) \tag{2}$$

which attains values in $\mathbb{R}$. The output space ($\mathbb{R}$) is equipped with a grid of "levels" $\{k\delta \mid k \in \mathbb{Z}\}$, where δ represents the (fixed) distance between levels. It is assumed that a sensor provides the value of y at times t for which

$$y(t) \in \{k\delta \mid k \in \mathbb{Z}\}. \tag{3}$$

This situation is visualised in Figure 2.

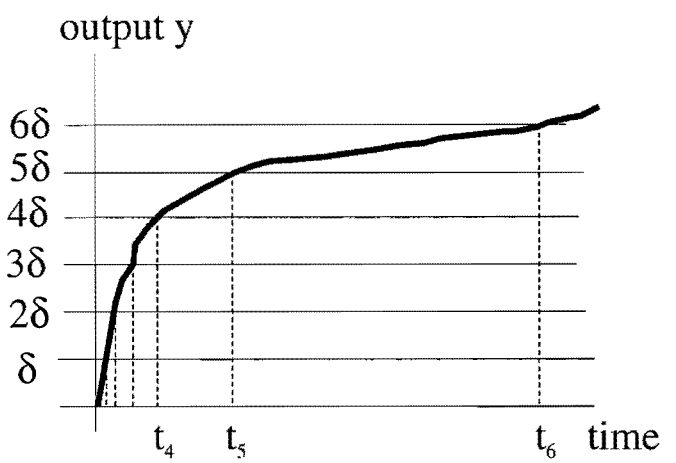

Figure 2: Measurements with a level sensor/encoder

A new measurement becomes available when the output $y(t)$ crosses one of the horizontal lines that are δ units apart (state-event). Note that the smaller the derivative of y is, the longer it takes before new information on the system becomes available. Note the difference with conventional sampling: the output $y(t)$ is available only at times t which are an integer-multiple of the sampling time (time-event).

The problem is to design a controller that produces the control u based on information of a state-event sensor of y such that the (continuous-time) output y tracks a given reference signal r in spite of the presence of disturbances d. In fact, the tracking error $e = y - r$ is required to meet the prior specified bounds

$$\max_{t\geq 0} \mid e(t) \mid = \max_{t\geq 0} \mid y(t) - r(t) \mid \leq \varepsilon \tag{4}$$

for $\varepsilon > 0$.

2.2 Test set-up

The test set-up (Figure 3) consists of two induction motors each driving a different load by means of a gear box (gear ratio i_{gear} is equal to 12.5 meaning that the motor axis turns 12.5 times faster than the load axis). One motor is the master (supposed to drive a conveyor belt) and the other motor is the slave (driving the sheet-feeder) in the sense that the slave motor position has to track the position of the master motor. In terms of the previous subsection this means that the system (1) describes the dynamics of the slave motor, the output $y = \theta_s$ $[rad]$ is the (angular) position of the slave motor axis and the reference $r = \theta_m$ $[rad]$ is the actual position of the master motor axis (In figure 3 $\theta_m = \theta_{mm}$ and $\theta_s = \theta_{sm}$. Furthermore, θ_{ml} $[rad]$ and θ_{sl} $[rad]$ denote the angular position of the load axis of the master and slave, respectively.)

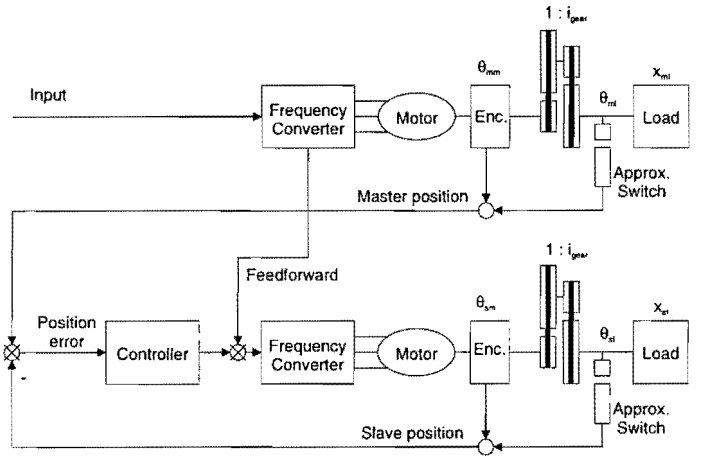

Figure 3: The test set-up

The positions of the motors are measured by encoders. The position of the master θ_m will be measured by a high resolution encoder with 1024 equidistant measurements per revolution yielding a resolution of $\delta_m := \frac{2\pi}{1024}$. The position of the slave will be measured by an encoder with N equidistant measurements per revolution of the motor axis. This means that in (2) the constant $\delta = \delta_s$ is equal to $\frac{2\pi}{N}$ $[rad]$.

The controller aims at regulating the slave motor such that the slave load axis is synchronised to the master load axis. The error on the load axis is required to stay between -0.1 rad and 0.1 rad. Incorporating the gear ratios gives a maximal allowed error between the position of the motor axes of slave and master of 1.25 rad. The problem is to design a controller such that

$$\max_{t\geq 0} | \underbrace{\theta_m(t) - \theta_s(t)}_{e_\theta(t)} | \leq \varepsilon = 1.25 \text{ rad} \tag{5}$$

irrespective of present disturbances and actuator limitations.

The disturbances of the system are mainly due to the varying loads of the motors. In the test-up a constant load is connected to the master motor. This corresponds to the normal operating conditions of the mailing system, because the load driven by the conveyor belt is constant or

slowly varying. The slave drives a so-called sheet-feeder. The sheet-feeder consists of a large metal drum, that is rotated by the motor. To this drum a set of grippers, intended for grabbing a brochure, is connected. In a mailing system the brochure is transported over the metal drum to a conveyor belt (lug chain), where the brochure is released. The grippers are pressed to the drum by a set of springs. These springs are strained and released via a camshaft that is attached to the metal drum. The pressing and releasing of the various springs result in a varying load torque. As all the operations are cyclic with the rotation of the drum, the disturbing torque that is exerted to the motor depends on the position θ_{sl} $[rad]$ of the load axis (the drum). In Figure 4 the torque as a function of the load axis position θ_{sl} is given.

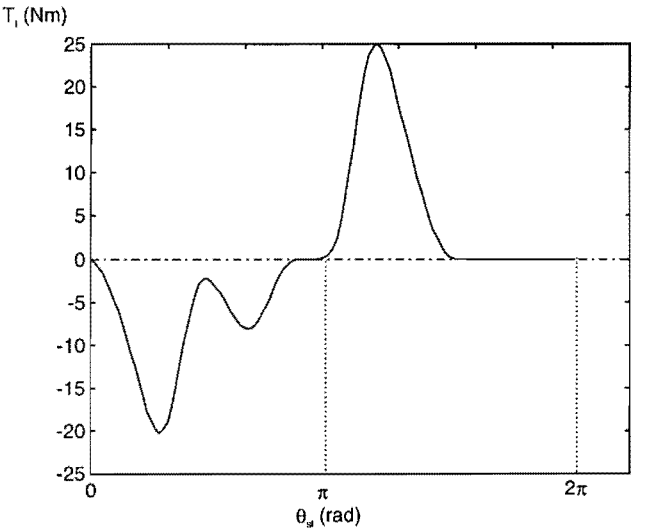

Figure 4: Sheet-feeder torque (fluctuating part)

This torque function was calculated from the spring constants and verified by measurements. To obtain the disturbance torque that is exerted on the motor axis, it has to be divided by the gear ratio $i_{gear} = 12.5$. Next to this fluctuating torque (depicted in Figure 4) a constant torque is present due to Coulomb friction. Taking this constant and fluctuating torque together results in the disturbance $d(t)$ in (1).

The induction motors are powered by a frequency converter (Figure 3). The frequency converter generates three sine waves, which drive the motor. The frequency and amplitude of the sine waves are linear to the input voltage of the frequency converter. To bound the slip (the difference between the stator frequency and the mechanical frequency) in the motor, a rate limiter is included in the frequency converter (minimum/maximum rate ± 35 $[Hz/s]$). Furthermore, the magnitude of the output frequency is limited to 70 $[Hz]$. As will be shown later, the rate limiter poses severe limitations to achieve a high bandwidth.

As a model for the slave motor and the mechanical system a simple third order model is used

(Leonhard, 1984) given by the following state space description

$$\dot{\theta}_s(t) = \omega_s(t) \tag{6a}$$

$$\dot{\omega}_s(t) = \frac{1}{J}[T(t) - B\omega_s(t) - d(t)] \tag{6b}$$

$$\dot{T}(t) = \frac{1}{\tau}[-K_t\omega_s(t) - T(t) + K_tK_fu(t)], \tag{6c}$$

where θ_s $[rad]$ is the position of the slave motor axis, ω_s $[rad/s]$ the speed of the motor axis, T $[Nm]$ the torque generated by the motor, u $[rad/s]$ is the reference frequency coming from the frequency converter (control input) and d $[Nm]$ the disturbance torque generated by the sheet-feeder. In this model the frequency converter is assumed to be linear with a gain K_f. The torque slip-angle curve of the induction motor is linearized by the factor K_t $[Nms/rad]$. J $[kg\,m^2/rad]$ is the inertia of the rotor plus load and B $[Nms/rad]$ is the mechanical damping. The constant τ $[s]$ represents the electrical time constant in the motor (Leonard, 1984). Using the motor name plate data and various measurements, the model parameters were estimated for the slave motor using techniques of Gorter (1997) resulting in $K_t = 0.35$ $[Nms/rad]$, $K_f = 46.3$, $\tau = 0.05$ $[s]$, $J = 8.5\ 10^{-3}[kgm^2]$ and $B = 9.8\ 10^{-3}$ $[Nms/rad]$. Finally, note that equations (6) are of the form (1). The measurement is $y(t) = \theta_s(t)$.

3 Conventional (synchronous) control

As is observed in Figure 3, feed-forward of the signal coming from the frequency converter of the master to the slave frequency converter is applied. In the ideal case that both motors are identical and driving the same load, no additional control action will be necessary to keep the motors running synchronously. In the nonideal case, a feedback controller is needed to reduce the position error between master and slave. The feed-forward will be used in all controller designs, only the feedback controller will vary.

To compare the performance of classical approaches to the control design with asynchronous measurements, a standard PID-controller with a fixed sample rate is designed. The PID controller has been designed using standard root-locus techniques (see e.g. Franklin et al., 1994). From the Bode magnitude plot drawn in Figure 5, the closed loop disturbance rejection (effect of d on θ_s) can be compared with that of the uncontrolled process.

At low frequencies good disturbance rejection is obtained at the cost of some magnification at frequencies between 10 and 50 $[rad/s]$. It was tried to increase the disturbance rejection by using a high order H_∞-controller. It was found that the actuator rate limitation prevents further improvements (Van Zijl, 1997). Hence, the actuator is the bottle neck in achieving high bandwidth. To test the controller on the real system, it was implemented using a digital signal processor. The continuous controller was converted to discrete time with a sample frequency of 2 kHz. To avoid wind-up of the integrative action, the conditioning technique was used (Peng et al, 1996).

As stated in the description of the test set-up, the resolution of the position measurement of the slave (θ_s) and master motor axis (θ_m) are $\delta_s = \frac{2\pi}{N}$ and $\delta_m = \frac{2\pi}{1024}$, respectively. The measured

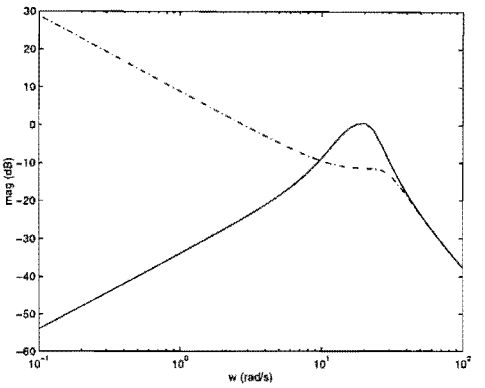

Figure 5: Bode magnitude plot of disturbance rejection ($\frac{\theta_s}{d}$) in controlled (solid) and uncontrolled process (dashed).

signals $\theta_{s,mea}$ for the slave and $\theta_{m,mea}$ for the master. These signals are piecewise constant with discontinuities appearing at the moment that new measurements become available. Formally,

$$\theta_{s,mea}(t) = k\delta_s, \text{ if } k\delta_s \leq \theta_s(t) \leq (k+1)\delta_s \tag{7}$$

and

$$\theta_{m,mea}(t) = k\delta_m, \text{ if } k\delta_m \leq \theta_m(t) \leq (k+1)\delta_m. \tag{8}$$

It is easily derived that the difference between the measured signals and the real signals satisfy the following relations.

$$0 \leq \theta_s(t) - \theta_{s,mea}(t) \leq \delta_s \tag{9}$$

$$0 \leq \theta_m(t) - \theta_{m,mea}(t) \leq \delta_m \tag{10}$$

The measured position error at time t, $e_{\theta,mea}(t) := \theta_{m,mea}(t) - \theta_{s,mea}(t)$ differs from the real position error $e_\theta(t)$. The error can be bounded by using the above inequalities.

$$-\delta_s \leq e_\theta(t) - e_{\theta,mea}(t) \leq \delta_m \tag{11}$$

Hence, the maximum error is equal to $\max(\delta_s, \delta_m)$. The discretized PID-controller (updated at a constant control rate of 2 kHz) is based on the measured position error.

In Figure 6, the resulting tracking errors are given for the experimental set-up using 1024 measurements per revolution for both the motor axis of the master and the slave $\delta_m = \delta_s = \frac{2\pi}{1024} = 6.14 \cdot 10^{-3}$ $[rad]$.

In this figure the position error on the motor axes is given for different motor speeds (42.5 rad/s, 138 rad/s, 180 rad/s and 225 rad/s, respectively). As can be seen from this figure, the position error lies within the required error bound of 1.25 rad for all the considered speeds. The small fluctuations are caused by the position dependent disturbance of the sheet-feeder. Since the frequency of this periodic disturbance depends on the motor speed, the frequency of the fluctuations differ for varying speeds. These fluctuations do not interfere with the correct operation of

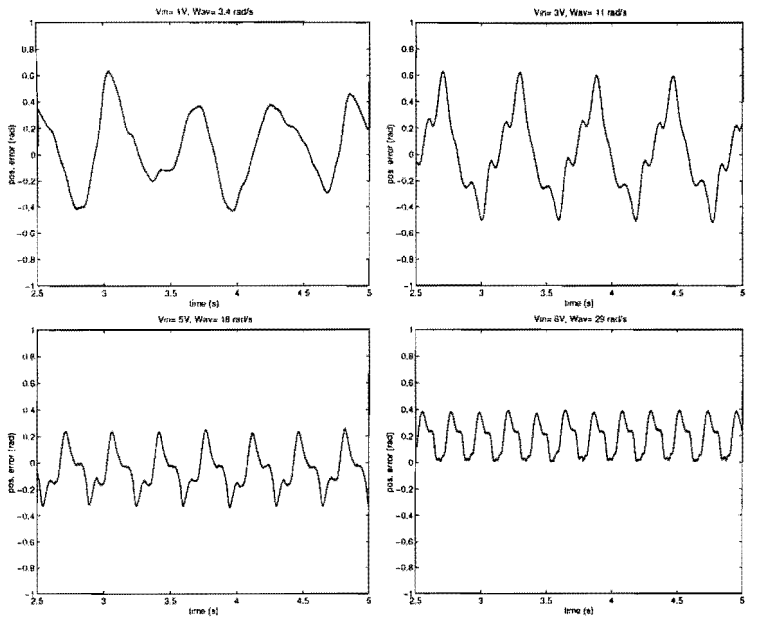

Figure 6: Position error for different motor speeds.

the mailing machine. If the fluctuations need to be attenuated more, the bottle neck will be the rate limiter that prevents the counteraction for the quickly varying disturbance (as mentioned before).

Note that expensive encoders are needed in this scheme. To reduce the costs of the complete mailing machine, the influence of a lower encoder resolution is investigated by lowering number of pulses per revolution of the slave motor axis to N pulses corresponding to a resolution of $\delta_s = \frac{2\pi}{N}$ $[rad]$. The same PID control scheme has been used where $e_{\theta,mea}$ (with N measurements per revolution of the slave motor axis) is taken as input of the controller. In Figure 7, the real experimental position errors are given for $N = 1$.

Most striking is that the average value of the position error deviates considerably from zero. Furthermore, the fluctuations around the average value of the position error are quite large (up to 2 $[rad]$ for low speeds) in comparison with the high encoder resolution case. One reason for a nonzero average of the position error is that although the real position error may be exactly equal to zero, the measured position error $e_{\theta,mea}$ is not equal to zero due to the updating mechanism. This phenomenon is displayed in figure 8. The signals θ_m, θ_s and $\theta_{s,mea}$ are drawn in the upper part of the figure and the difference $e_{\theta,mea}$ in the lower part. We assume that the real position error is equal to zero, i.e. $\theta_m = \theta_s$. As the master encoder has a very high resolution, the position measurement $\theta_{m,mea}$ is regarded to be equal to θ_m. Hence, the measured slave position will change in discrete steps of hight $\frac{2}{\pi}$ ($N = 1$). Obviously, $e_{\theta,mea}$ will have a (strictly) positive average value driving the real position error away from zero. Furthermore, the quickly varying signal $e_{\theta,mea}$ passes through the controller to the frequency converter. Due to the rate limiter the output of the frequency converter cannot follow this signal and will lag behind (see Van Zijl, 1997), which may deteriorate the position tracking even further.

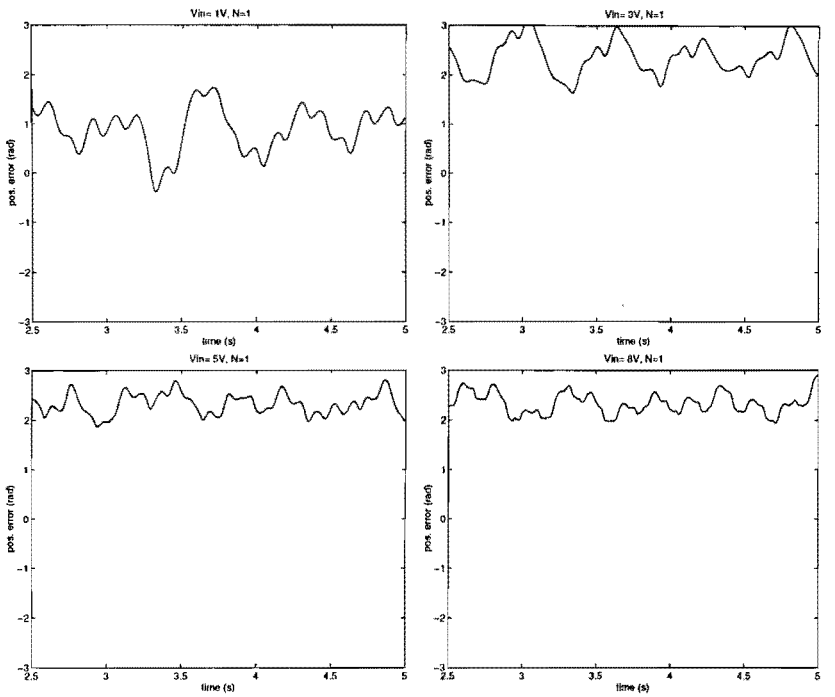

Figure 7: Position error using one measurement per revolution.

For $N = 1$ the control algorithm is based on a measured position error signal of the real position error that will have discretization errors up to $\delta_s = 2\pi$ $[rad]$ (see (11). Of course, one cannot expect any controller (implemented as above) to meet the specifications with such poor measurements. There is a need for alternative methods which are suitable for state-event sensors.

4 Asynchronous measurements

A first improvement of the above control scheme lies in a better use of the measured position error. In the previous section it was argued that the difference between the measured error and the real error can increase up to $\frac{2\pi}{N}$ $[rad]$ in case of N pulses per revolution of the motor axis. However, at certain time instants the position error can be determined with an accuracy equal to the high resolution of the master encoder (i.e. $\frac{2\pi}{1024}$ $[rad]$). At the times the slave position measurement become available, the slave position is exactly known. Denote the collection of these time instants by $\mathcal{D}$, i.e.

$$\mathcal{D} = \{t \geq 0 \mid \theta_s(t) = k\delta_s \text{ for some } k \in \mathbb{Z}\}. \tag{12}$$

Hence, $\theta_{s,mea}(t) = \theta_s(t)$ for all $t \in \mathcal{D}$. Using the error bounds for the master motor position as in (10), it is evident that

$$0 \leq e_\theta(t) - e_{\theta,mea}(t) \leq \delta_m \quad \text{for all } t \in \mathcal{D}. \tag{13}$$

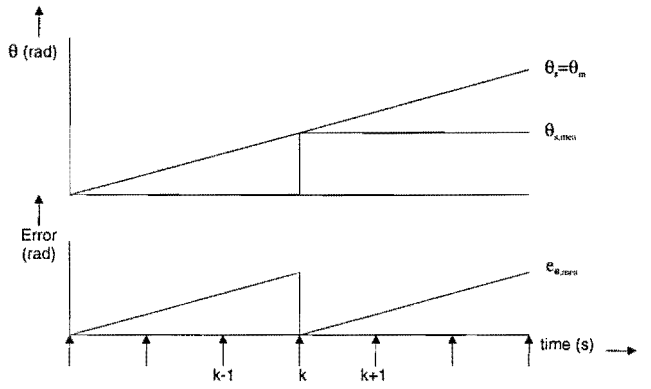

Figure 8: The signal $e_{\theta,mea}$ for low encoder resolution

Hence, for time instants $t \in \mathcal{D}$, the accuracy of the measurement is equal to the master encoder resolution $6.14 \cdot 10^{-3}[rad]$ *independent of the number* N *of encoder pulses per revolution of the motor axis of the slave.* The advantage of a larger N is that more measurements are available in the same time span. Note that the instants at which a slave position measurement becomes available are not equally distributed in time. In fact, they are triggered by state-events. Clearly, for higher velocities more measurements become available per time span. This method of measuring is called 'asynchronous measurement.' New control strategies based on asynchronous measurement will be proposed in the next section.

5 Hybrid control

In the hybrid control scheme, the controller output is still updated at a fixed rate of 2 kHz resulting in the (controller-)sample times $\{t_i\}_{i\in\mathbb{N}}$ with $t_i = 5 \cdot 10^{-4}\ i\ [s]$, $i \in \mathbb{N}$. The error signal used as input of the PID-controller is kept constant between two subsequent time instants contained in $\mathcal{D}$. This means that the input, used by the controller to update its control value at time t_i, is

$$e_{\theta,mea}(t') \text{ with } t' = \max\{t \in \mathcal{D} \mid t \leq t_i\}.$$

Hence, only at times $t \in \mathcal{D}$ the input signal for the controller is updated to the value $e_{\theta,mea}(t)$ and it is kept constant until the next time instant in $\mathcal{D}$.

Since the signal structure of the controller output (triggered by time-events, fixed rate) and its input (state-events, varying rate) are essentially different, this mixed control structure is called 'hybrid.' After fine tuning of the PID-controller, the obtained experimental results are shown in Figure 9 for the various reference speeds and with $N = 1$.

If this figure is compared to Figure 6, where the full encoder resolution is used, it can be seen that the lower encoder resolution does not result in larger position errors using the technique described above. This seems quite remarkable, but can be explained by the fact that the PID-controller only attenuates the low frequency components of the disturbance (Figure 5). The

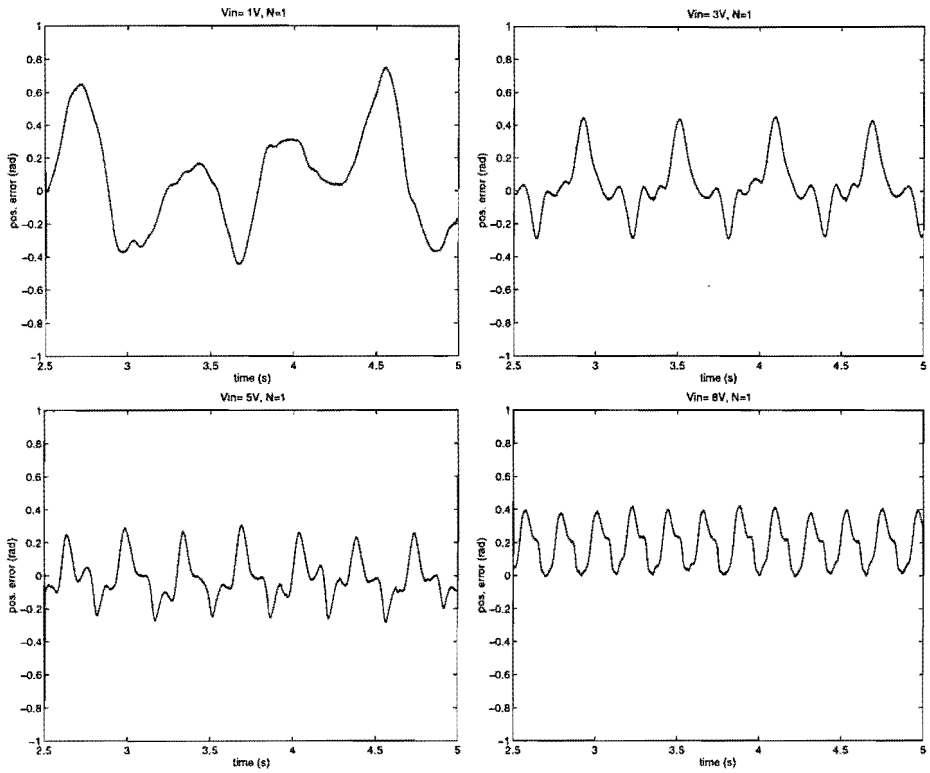

Figure 9: Real experimental position error with a hybrid controller.

position error estimation procedure provides a good fit to the real position error for these low frequencies and as a consequence the hybrid controller does not display poorer performance in comparison with the control structure of section 3 with high encoder resolutions. Furthermore, in contrast with the implementation in section 3, the input of the controller is equal to zero in case that the position error is zero, i.e. $\theta_s = \theta_m$ (See Figure 8). This method yields also a slower varying control signal that prevents saturation of the rate limiter.

The hybrid approach is related to the work of Philips and Tomizuka (1995), who also use a fixed control rate and a asynchronous update of the observer. Philips and Tomizuka propose to estimate the complete state in (6) (i.e. the position θ_s, the velocity ω_s and the torque T) by using a Luenberger observer to predict the intersample behaviour based upon a model of the system. However, the scheme presented here is simpler, since a complete state observer is not needed. Furthermore, the method in Philips and Tomizuka (1995) calls for the on-line computation of matrix exponentials in a relative short time frame, which requires fast processors.

6 Asynchronous control

In the asynchronous control scheme both the position error estimate and the control signal will be updated at time instants at which the slave position measurement becomes available. As mentioned in the introduction, for an asynchronous controller the classical design theory does

not apply. The reason is that a standard assumption in the literature on sampled-data systems is that the control update times are equally spaced along the time axis (synchronously distributed). A new design technique is needed and the work presented here can be seen as a first step in filling towards bridging the gap between control of on sampled-data systems and control of systems with level sensors. Our approach is based on transforming the control problem into a form that is suitable for the classical control techniques.

6.1 Transformation

The design technique is based on the observation that although the measurements and control updates are not equally spaced along the time axis, they are equally spaced (i.e synchronous) in the position of the motor axis, because the notches (markers) of the encoder have an equidistant distribution along the motor axis of the slave. The model description (6) with time being the independent variable will be transformed to an equivalent model in which the slave motor position is the independent variable. This yields a new system description in which the measurement instants are equidistant in the new independent variable, which is the position of the motor axis.

The transformation from the time domain (t) to the position domain (θ_s) can be made by recalling the following relation from (6):

$$\frac{d\theta_s}{dt}(t) = \omega_s(t). \tag{14}$$

The idea is to no longer view the angle θ_s as a function of time t, but instead time t as a function of angular position θ_s. However, to interchange the roles of time t and position θ_s, there must exist a one-to-one relation between the two variables. It will be shown that such a relation exists under a suitable assumption. In the meantime, the notation $t(\theta_s)$ is used to denote the time at which the slave reaches position θ_s. Similarly, $\omega(\theta_s)$ will denote the angular velocity of the slave motor axis when the axis is at position θ_s. Moreover, θ_s will be replaced by θ for brevity.

If $\omega_s(t) \neq 0$ holds, (14) can be rewritten as

$$\frac{dt}{d\theta}(\theta) = \frac{1}{\omega(\theta)} \tag{15}$$

Under the assumption that $\omega_s(t) \neq 0$ for all $t > 0$, such a one-to-one correspondence between the position of the slave motor axis θ and the time t indeed exists. The interpretation of the requirement $\omega_s(t) \neq 0$ is that the slave motor may not change its direction of movement.

Using (15) the system description (6) can be rewritten as:

$$\frac{dt}{d\theta}(\theta) = \frac{1}{\omega(\theta)} \tag{16a}$$

$$\frac{d\omega}{d\theta}(\theta) = \frac{1}{J}\left[\frac{T(\theta)}{\omega(\theta)} - \frac{d(\theta)}{\omega(\theta)} - B\right] \tag{16b}$$

$$\frac{dT}{d\theta}(\theta) = \frac{1}{\tau}\left[K_t K_f \frac{u(\theta)}{\omega(\theta)} - \frac{T(\theta)}{\omega(\theta)} - K_t\right] \tag{16c}$$

where $T(\theta)$, $d(\theta)$, $u(\theta)$ denotes the torque generated by the slave motor, the disturbance torque exerted at the motor and the control value, respectively, when the slave position is equal to θ. There is some abuse of notation here. However, the argument of the quantities will clarify whether the quantity is considered as a function of time or as a function of the slave position. Note that the time t is now a component of the state of the model. The output of this new description is selected to be the time $t(\theta)$.

$$y(\theta) = t(\theta) \tag{17}$$

Note that the output is only available at discrete time instants for which θ is equal to a multiple of δ_s.

The position error between the master and the slave motor axis in the time domain can be related to the time difference between the arrival of the master and slave at the same position. Formally, this last quantity equals $e_t(\theta) = t_s(\theta) - t_m(\theta)$, where $t_s(\theta)$ and $t_m(\theta)$ denote the time instants at which the slave and master motor axis, respectively, reach position θ. The subscript s will be omitted in case the slave dynamics is considered. For instance, $t(\theta)$ means $t_s(\theta)$. In Figure 10, a possible position characteristic for the master (θ_m) and slave motor (θ_s) is drawn.

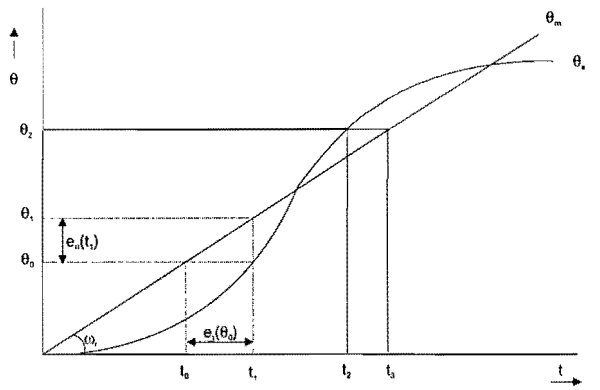

Figure 10: Master and slave position

From Figure 10, the following relationship between the position and the time error can be derived.

$$\frac{e_\theta(t_1)}{e_t(\theta_0)} = \omega_r, \tag{18}$$

where ω_r is the master motor (reference) speed. This relation is exact as long as ω_r is constant. If ω_r is not constant, (18) can be used as an approximation. Note that the master motor normally drives a conveyor belt in a mailing system. Since the fluctuations in the load of the conveyor belt are relatively small, the master motor will run at a constant speed (or with a slowly varying speed) under normal operating conditions and thus (18) will hold. From (18), it is evident that reducing $e_\theta(t_0)$ is equivalent to reducing $e_t(\theta_0)$. The control objective can thus be reformulated as follows: design a controller H_c in the position domain that maps $e_t(k\delta_s)$, $k \in \mathbb{N}$ (note that the sample interval equals δ_s) to control inputs $u(\theta)$ such that the time error $e_t(\theta)$ is as small as possible.

6.2 Design

The control problem that was asynchronous in the time domain has now been transformed into a synchronous control problem in the position domain. The price paid is that the controller design becomes more complicated as the process model given in (16) is nonlinear. The control of a nonlinear system is not straightforward although more and more nonlinear control design techniques appear in the literature. An approach to the control design for a system as in (16) is linearizing around an 'equilibrium' trajectory corresponding to a master motor speed that is constant (normal operating conditions). In this case, a steady state trajectory is $(t, \omega, d, T, u) = (\frac{1}{\omega_r}\theta, \omega_r, \bar{d}, B\omega_r + \bar{d}, \frac{1}{K_f}[\omega_r + \frac{B\omega_r}{K_t} + \frac{\bar{d}}{K_t}])$ and the variations around this equilibrium trajectory are denoted by $(\tilde{t}, \tilde{\omega}, \tilde{T}, \tilde{d}, \tilde{u})$. Here $\bar{d}$ denotes the mean value of the disturbance d. Hence,

$$t = \frac{1}{\omega_r}\theta + \tilde{t} \tag{19a}$$

$$\omega = \omega_r + \tilde{\omega} \tag{19b}$$

$$T = B\omega_r + \bar{d} + \tilde{T} \tag{19c}$$

$$d = \bar{d} + \tilde{d} \tag{19d}$$

$$u = \frac{1}{K_f}[\omega_r + \frac{B\omega_r}{K_t} + \frac{\bar{d}}{K_t}] + \tilde{u}. \tag{19e}$$

Around this equilibrium trajectory, the linearized dynamics are

$$\frac{d\tilde{t}}{d\theta} = -\frac{1}{\omega_r^2}\tilde{\omega} \tag{20a}$$

$$\frac{d\tilde{\omega}}{d\theta} = \frac{1}{J\omega_r}[-B\tilde{\omega} + \tilde{T} - \tilde{d}] \tag{20b}$$

$$\frac{d\tilde{T}}{d\theta} = \frac{1}{\tau\omega_r}[-K_t\tilde{\omega} - \tilde{T} + K_tK_f\tilde{u}] \tag{20c}$$

$$\tilde{y} = \tilde{t} \tag{20d}$$

where all signals are functions of θ.

A feedback controller needs to be designed whose output defines the first order variation $\tilde{u}$. By (19e) this controller output has to be added to the equilibrium value $\frac{1}{K_f}(\omega_r + \frac{B\omega_r}{K_t} + \frac{\bar{d}}{K_t})$ to generate the control input u. The feed-forward signal coming from the master frequency converter takes care of the major part of this constant equilibrium value. The remaining part must be regulated by the feedback controller.

A minimal requirement for the feedback controller is that for all relevant reference speeds ω_r the closed loop system (of the linearized system) is stable. Furthermore, it is desirable that the relative damping of the closed loop poles are not too sensitive for variations in the reference speed ω_r. This will yield the same behaviour in the time domain for all reference speeds, as will become clear later.

To proceed, the system description will be discretized in the position domain and a controller will be designed using the root locus method. A PI-controller with the following transfer function is

designed.

$$H_c(z^*) = K_c \frac{z^* - a}{z^* - 1} \tag{21}$$

Note that z^* is used instead of z to stress that the discretization is in the position domain. The location of the zero and the gain are chosen as $a = 0.9$ and $K_c = 41$ such that the system shows a desirable and stable behaviour at the largest value of ω_r (about 375 $[rad/s]$). This controller is applied to (20) for other reference speeds ω_r to evaluate whether the behaviour of the closed loop system is acceptable.

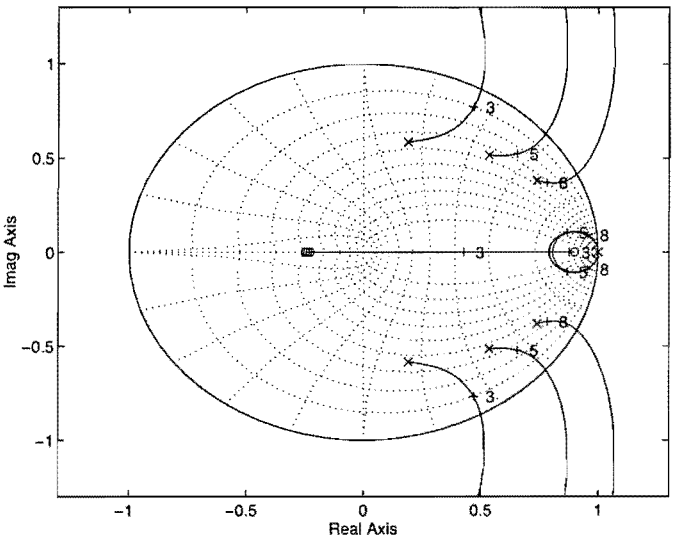

Figure 11: Root loci for varying ω_r and constant controller

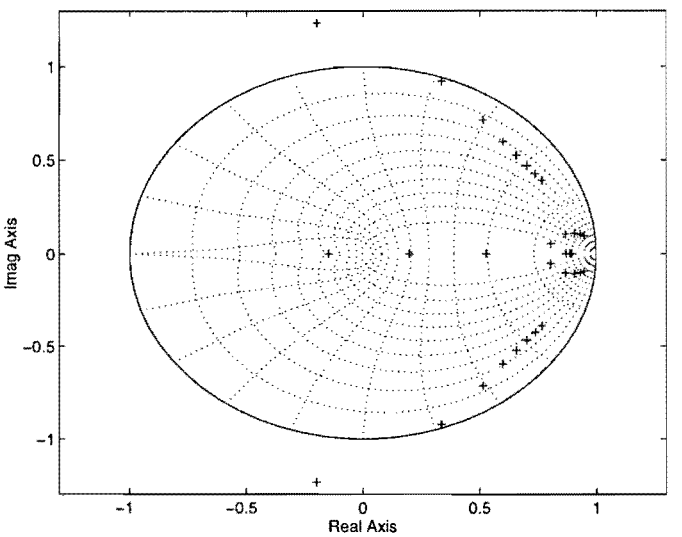

Figure 12: Pole locations for varying ω_r and constant controller

In Figure 11 the root loci are plotted for three values of ω_r (from left to right corresponding to ω_r equal to 138, 225 and 363 $[rad/s]$, respectively and the input voltages to the master frequency

converter 3, 5 and 8 [V], respectively). The closed loop poles corresponding to $K_c = 41$ are denoted by '+'-marks and labelled by the input voltages. With decreasing ω_r the amount by which the closed loop roots are shifted from their original value increases. The relative damping of these poles decreases with decreasing ω_r resulting in different closed loop behaviours. In Figure 12, the closed loop poles are plotted for several intermediate reference speeds ω_r (ranging from 75 to 375 [rad/s]) with gain equal to $K_c = 41$ for the controller. One observes that for low speeds the poles are even outside the unit circle resulting in unstable behaviour. It is evident, that this controller is unacceptable. As the value of the overall controller gain K_c determines the amount by which the poles shift over the loci, instability of the system can be circumvented by choosing K_c sufficiently small. However, a drawback is that the open loop poles in 1 stay close to the unit circle resulting in a slow closed loop system. Furthermore, it can not be prevented, that the relative damping changes for different reference speeds.

From (20) is evident that the process poles depend on ω_r. Therefore, a fixed controller as above will not give satisfactory results for all ω_r. A possible solution is to make the controller dependent on ω_r, thus neutralising the dependency of the process on ω_r. If K_c is a function of ω_r then this could reduce the effect of changing relative damping and instability. From the discussion in the previous paragraph, it is clear that K_c should be smaller for smaller values of ω_r. The gain K_c is selected to be proportional to ω_r according to $K_c(\omega_r) = 3.3\omega_r$. Again the root loci were drawn for the same values of ω_r as before (Figure 13). The '+' refers again to the closed loop poles for $K_c(\omega_r) = 3.3\omega_r$. The relative damping of the complex conjugate poles is almost constant and the system does not become unstable for small ω_r anymore. Stability is even ensured for all values of ω_r. This is stressed additionally by Figure 14, where the closed loop poles are drawn for the same intermediate values as in Figure 12.

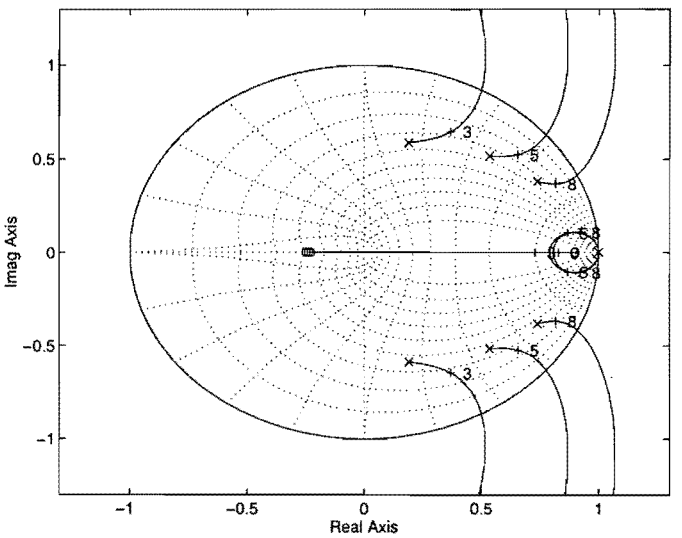

Figure 13: Root loci for varying ω_r and ω_r-dependent controller

For the reference speeds ω_r equal to 138, 225, 363 [rad/s] step responses are drawn in the upper part of Figure 15. A unit step on such a system means that instantaneously the master position (the reference) reaches the next positions exactly one second later. Consequently, the step response displays the time variation (with respect to the equilibrium trajectory $\frac{1}{\omega_r}\theta$) at

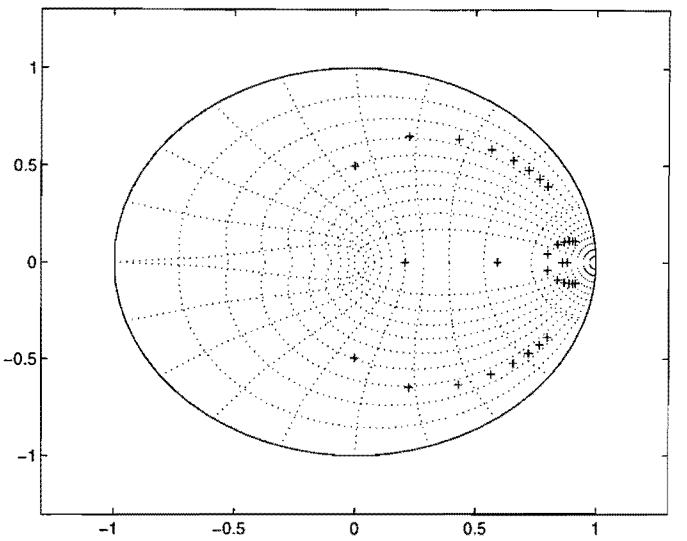

Figure 14: Pole locations for varying ω_r and ω_r-dependent controller

which the slaves reaches a certain position. The step heights for different reference speeds are normalised by multiplying with $\frac{1}{\omega_r}$ to get a step of 1 $[rad]$ on the position error $e_\theta(t)$. In the lower part of Figure 15, the resulting position errors $e_\theta(t)$ are drawn with respect to time. The position errors stay within the bound of 1.25 $[rad]$. Notice also that the settling time is almost equal for all the three cases. This is caused by the fact that for increasing reference speeds, the natural frequency of the closed loop of the linearized transformed system decreases proportionally while the relative damping stays the same. In the position domain the sampling instants are equally separated for varying reference speeds (equal to 2π). In the time domain, the time between measurements is proportional to the inverse of the reference speeds; the higher the reference speed, the smaller the time that the next measurement becomes available. Hence, the effect of decreasing natural frequencies is cancelled by the effect of closer 'sampling instants' in the time domain. As a consequence, the closed loop systems in the time domain are equally fast. This is the reason why a closed loop system with the same relative damping for varying speeds was preferred. The small differences in the time responses are caused by the fluctuations in the poles close to one.

The controller performance is evaluated by drawing the Bode amplitude plots of the transfer function from the disturbance $\tilde{d}$ to the systems output $\tilde{y}$ using techniques of Åström and Wittenmark, 1984 to incorporate also the intersample behaviour. The Bode plot of the closed loop system (in the position domain) is drawn in Figure 16. The value $10^0 = 1$ on the x-axis complies with one revolution of the motor axis. Drawn from top to bottom are the closed (solid lines) and open loop (dashed lines) magnitude plots complying with the reference speeds 43, 138, 225 and 363 $[rad/s]$, respectively. The controller has most influence for low frequencies. In general, the larger the reference speed, the larger the disturbance rejection.

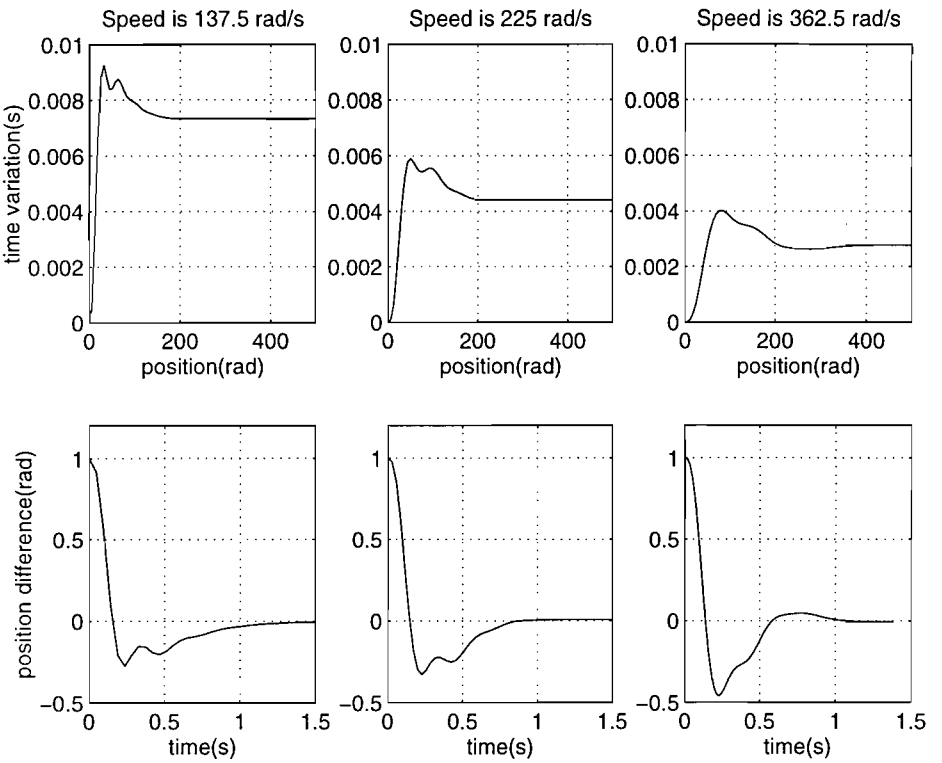

Figure 15: Step responses of the closed loop system for varying reference speeds and the transformed position errors.

6.3 Implementation

An implementation problem arises if the above controller has the time difference directly as its input. A first problem is that one needs to store the time instants at which the master and slave reach certain positions. If the slave is lagging behind ($(k-1)\delta_s \leq \theta_s(t) \leq k\delta_s$ and $(l-1)\delta_s \leq \theta_m(t) \leq l\delta_s$ for $l \geq k$), then all the times $t_m(k\delta_s)$, $t_m((k+1)\delta_s)$, ..., $t_m(l\delta_s)$ must be stored. The reason is that when the slave reaches one of the positions $k\delta_s, \ldots, l\delta_s$, the times between the arrival of master and slave must be subtracted to get the time error. A more severe problem arises when the slave is ahead of the master. The value of $e_t(k\delta_s)$ is not easily retrieved in this case. If the slave is ahead of the master and reaches the position $\theta_2 = k\delta_s$ at time t_2 (see Figure 10), the master will reach the position $k\delta_s$ at some time instant t_3 that lies in the future (after time instant t_2). Hence, $e_t(k\delta_s) = t_3 - t_2$ cannot be determined at time t_2. Consequently, $e_t(k\delta_s)$ is not known at time instant t_2, because $t_m(k\delta_s)$ is not available (the trajectory of the master is not known a priori). A solution for both problems is estimating $e_t(k\delta_s)$ by using (18) to convert the position error to the time error. This approximation is exact if the reference speed ω_r is constant. This method results in the implementation depicted in Figure 17 (b). Note that the analysis and design has been performed in the position domain (Figure 17 (a)), but the actual implementation is, of course, in the time domain.

In view of Figure 17 (b), (21) and the definition of the gain $K_c(\omega_r) = 3.3\omega_r$, it becomes clear that

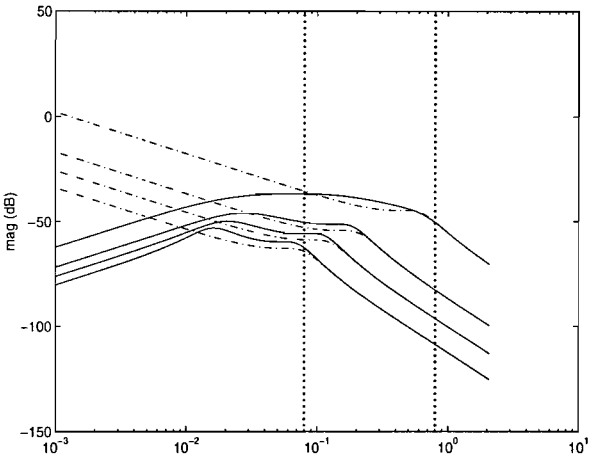

Figure 16: Bode plot disturbance rejection of closed and open-loop system, for various values of ω_r

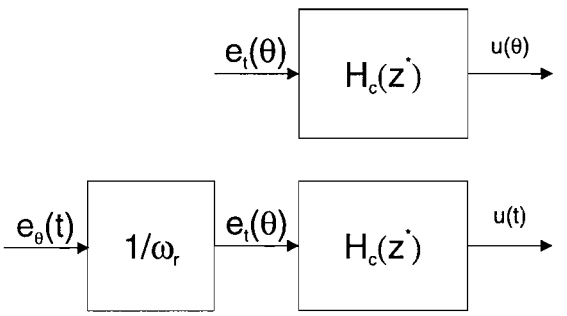

Figure 17: (a) Analysed controller (b) Actual implementation

the factor ω_r in the controller cancels out the $\frac{1}{\omega_r}$ multiplication needed to convert the position error to the time error. The overall control scheme is therefore no longer dependent on ω_r and the implementation of the controller is of the following simple form. Let $\mathcal{D}$ (see Section 4) be equal to $\{t_k\}_{k\in\mathbb{N}}$. The control value $\tilde{u}$ (see (20)) has to be updated at time t_k according to

$$\tilde{u}(t_k) = \tilde{u}(t_{k-1}) + 3.3e_{\theta,mea}(t_k) - 0.9e_{\theta,mea}(t_{k-1}), \tag{22}$$

which is a simple PI-structure for which the updates are triggered by state events. Hence, each time when a new slave measurement becomes available, the position error is calculated with an accuracy of $\frac{2\pi}{1024}$ and the control value is updated according to (22). Observe that there is no need for a speed observer of the master motor in order to implement (22). By (19e) the feedforward term (see Figure 3) has to be added to $\tilde{u}$ to obtain the control input u.

6.4 Validation

The designed asynchronous controller has been experimentally validated on the test set-up (Figure 18). For the reference speeds 42.5, 138, 225 and 363 $[rad/s]$ the position errors are

plotted. As expected from the Bode plots, it is observed that the disturbance rejection is better for higher speeds, resulting in smaller position errors. Observe that the maximum allowable error of 1.25 rad is not exceeded and thus the designed controller satisfies the required specifications.

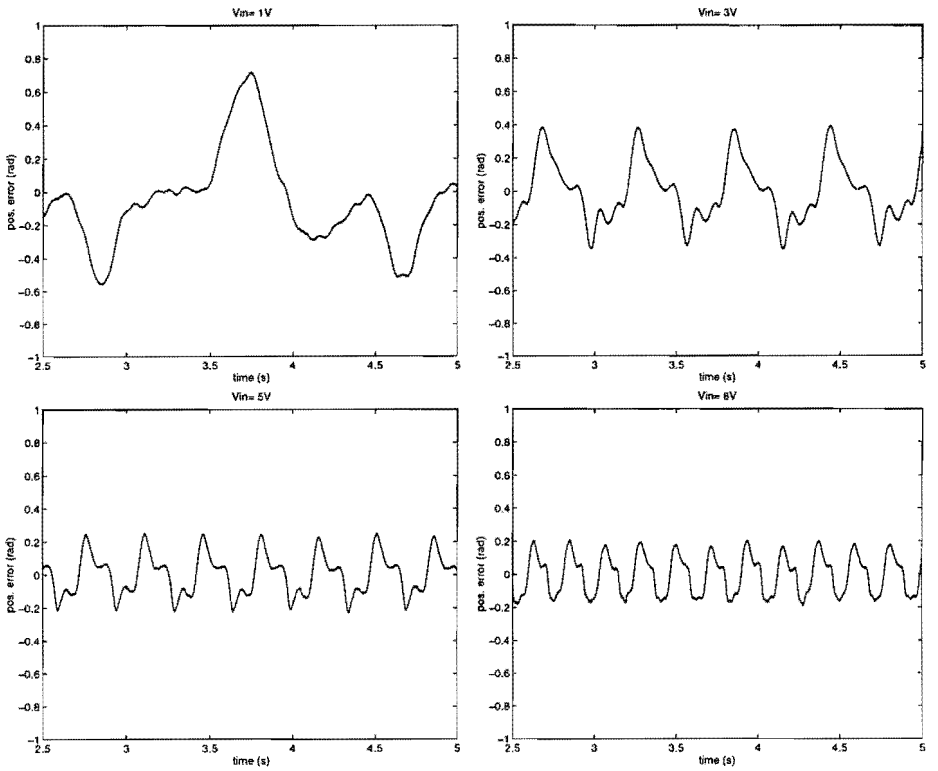

Figure 18: Position error for asynchronous control using 1 pulse per revolution.

7 Practically relevant test

Both the hybrid and asynchronous controller have been evaluated during the start-up procedure of the test set-up of the mailing system.

Starting up the mailing system is done on at least a daily basis. In this case, the master motor speed increases from 0 to 371 $[rad/s]$. Due to the gear ratio the load axis speed increases to 29.6 $[rad/s]$ corresponding to the normal operation speed of the mailing system of 17000 products per hour.

In Figure 19 the hybrid controller corresponds to the left pictures and the asynchronous controller to the right pictures. The top pictures display the speed trajectories for both the master (dotted) and the slave load axes (solid) with one measurement per revolution of the motor axis. The pictures in the center show that the position errors between master and slave on the motor axis and the lower pictures show the control values of the feedback controller in Volts. One observes that the mailing system can be brought to normal operating conditions in 4.5 seconds within the required position error bounds. Both developed controllers perform satisfactorily. Shutting the mailing system down shows similar results.

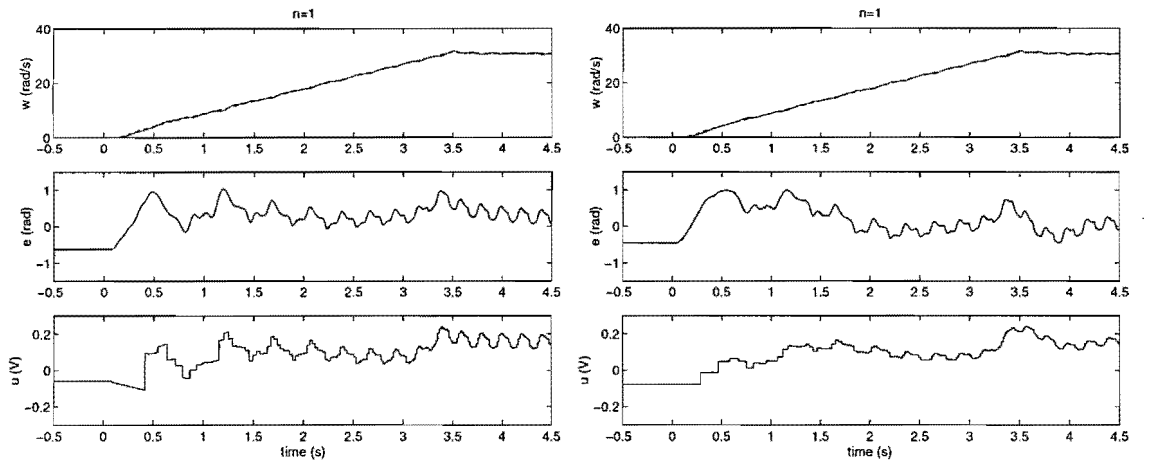

Figure 19: Starting up the mailing system with hybrid(left) and asynchronous(right) controller using 1 pulse per revolution.

8 Conclusions

In this paper, the design of a controller for synchronization of a master and slave motor in a mailing system has been studied. The position error between master and slave motor has to be kept within a priori specified bounds in spite of actuator limitations and present disturbances. Since the manufacturing costs of a mailing system should be kept low, the resolution of the encoder should be low and the resulting control structure simple. Otherwise, expensive encoders and fast processors would be required for the implementation.

The performance of the standard synchronous PI-controller suffices for high encoder resolutions for both the master and slave position measurement. However, the implementation of this controller for a mailing machine leads to very high costs, because every slave motor (sheet-feeder) should be equipped with an expensive high resolution encoder. To reduce the costs, it has been studied whether lower resolution encoders can provide a feasible performance. The sensor for the master is unchanged. The performance deteriorates dramatically if the same synchronous PI-controller is maintained. As a consequence, there is a need for new control techniques.

Two alternative control schemes, the hybrid and the asynchronous scheme have been developed. One of the main ideas was to use the position error measurements only when the low resolution encoder of the slave gives new information, i.e. crosses a sensor level. The accuracy of the measurement at these state-event times is equal to the accuracy of the high resolution encoder of the master. The hybrid controller keeps the input of the controller (the position error) constant in between measurement instants of the slaves, but maintains a fixed control rate. In this way the performance is greatly enhanced for low encoder resolutions. It has been shown that for the used test set-up a resolution of 1 measurement per revolution suffices. The design of the controller has been performed by standard root locus techniques. As the controller is a simple first order system, it is easy to implement. The measurement error, however should be updated asynchronously in time. This calls for some interrupt driven logic circuits in combination with a fixed timer to generate the output of the controller at fixed time intervals.

In the asynchronous control scheme both the measurement and control updates are not equidistant in time. Both updates are triggered by the same state-event. Since the literature provides only synchronous control design, the design of an asynchronous controller is not straightforward. To overcome this problem, the asynchronous linear (disregarding possible actuator saturations) system has been transformed into a synchronous nonlinear system. This system was linearized and a controller has been designed. This very simple controller has shown sufficient performance for resolutions as low as one measurement per revolution. In this case, the implementation requires interrupt driven logic circuits only.

One can imagine that the asynchronous control technique admits several extensions from a viewpoint of practical implementation. However, the followed design technique is only extendable if certain assumptions are met. Of course, the transformation is only applicable for one output that is measured asynchronously, since a state space description allows only one independent variable. The other measured outputs must be available at a state event. A second issue that prevents generalization, is the requirement $\omega(t) > 0$ for all $t > 0$. As soon as the velocity of the measured output changes sign, the one-to-one correspondence between the time variable and the position θ_s is lost. This problem can be resolved by making a reset of this correspondence. Then every sign switch of the velocity of the output would result in such a reset. This can be rather awkward, if many sign changes occur. In the master/slave synchronisation the reference signals are under normal operating conditions ramps that are strictly increasing. Hence, the situation of a sign switch of the slave position hardly occurs. A sign switch of the velocity means that the motor stops turning. Then, no new measurements become available and in the asynchronous control case no new control updates are made. In a industrial environment, some exception handling device has to be included, to guarantee that the slave motor starts running again.

However, in the considered set-up under nominal conditions this phenomenon is not observed. The only situation in which it might occur is when very fast changes in the reference speed ω_r are required.

Both the hybrid and the asynchronous controller comply to the demanded performance for very low encoder resolutions and at low cost. The choice between the asynchronous and the hybrid controller largely depends on the ease and cost of both implementations. If needed, the performance of the hybrid controller can be enhanced by using an observer type approach based on a model of the system as in Philips and Tomizuka (1995). However, the price paid to use that approach is that the control scheme will be more complex (fast processors, look-up tables, observers with time-varying gains have to be included). The performance of the asynchronous controller might be improved by using nonlinear control design techniques directly instead of linearization of the transformed system. This will be the object of further research.

References

Åström, K.J. and B. Wittenmark (1984). *Computer controlled systems: theory and design.* Prentice-Hall International Inc., Eaglewood Cliffs, N.J.

Bamieh, B.A. and J.B. Pearson, Jr. (1992). A general framework for linear periodic systems with applications to H_∞ sampled-data control. *IEEE Transactions on Automatic Control* Vol. 37, No. 4, pp. 418-435.

Chen, T. and L. Qiu (1994). H_∞ design of general multirate sampled-data control systems. *Automatica* Vol. 30, pp. 1139-1152.

Chiang, W.-W. (1990). Multirate state space digital controller for sector servo systems. *Proc. of the 29th Conference on Decision and Control, Honolulu, Hawaii.*

Franklin, G.F., J.D. Powell and A.E. Naeni (1994). *Feedback control of dynamic systems.* Addison-Wesley, Amsterdam.

Gorter, R.J.(1997). *Identification of physical parameters in an induction machine model.* Doctoral Dissertation, Eindhoven University of Technology, The Netherlands. Published by: CIP-Data Koninklijke bibliotheek, Den Haag, The Netherlands.

Hori, Y., T. Umeno, T. Uchida and Y. Konno (1991). An instantaneous speed observer for high performance control of DC servomotor using DSP and low precision shaft encoder. *Proc. of Fourth European Conference on Power Electronics and Applications, Firenze, Italy.*

Leonhard, W.(1984). *Control of electrical drives.* Springer Verlag Berlin, Heidelberg pp. 204-237.

Peng, Y., D. Vrancic and R. Hanus (1996). Anti-windup, bumpless and conditioned techniques for PID controllers. *J. Control Systems*, Vol. 16 No. 4, pp. 58-57.

Phillips, A.M. and M. Tomizuka (1995). Multirate estimation and control under time-varying data sampling with applications to information storage devices. *Proceedings of the*

1995 American Control Conference, Vol. 6, pp. 4151-5, American Autom. Control Council, Evanston, Illinois.

Sågfors, M.F. and H.T. Toivonen (1997). H_∞ and LQG control of asynchronous sampled-data systems. *Automatica*, Vol. 33, No. 9, pp. 1663-1668.

Voulgaris, P.G. (1994). Control of asynchronous sampled-data systems. *IEEE Transactions on Automatic Control.* Vol. 23, pp. 1451-1455.

Zijl, A. van (1997). *Asynchronous motor control.* Master of Science Thesis, Dept. of Electrical Engineering, Eindhoven University of Technology, The Netherlands.